# Simulating the Dynamics of the Primary Charge Separation Process in Bacterial Photosynthesis†

S. Creighton, J.-K. Hwang, and A. Warshel*
*Department of Chemistry, University of Southern California, Los Angeles, California 90007*
W. W. Parson
*Department of Biochemistry, University of Washington, Seattle, Washington 98195*
J. Norris
*Chemistry Division, Argonne National Laboratories, Argonne, Illinois 60439, and Department of Chemistry, University of Chicago, Chicago, Illinois 60637*

*Received October 13, 1987; Revised Manuscript Received December 4, 1987*

ABSTRACT: The mechanism of the initial electron-transfer process in the reaction centers of photosynthetic bacteria is examined by semiclassical trajectory calculations based on the crystal structure of reaction centers from *Rhodobacter sphaeroides*. The energies of the charge-transfer states in which an electron moves from a special pair of bacteriochlorophylls (P) to a neighboring bacteriochlorophyll (B) or bacteriopheophytin (H) are obtained by combining experimental standard redox potentials with calculated solvation free energies for the electron carriers in solution and in the reaction center. The free energies calculated for the reaction center include the effects of the protein residual charges, loosely bound water molecules, and the induced dipoles in the protein, in addition to the electrostatic interactions of the chromophores themselves. As the potential energies fluctuate during a trajectory, transitions from one state to another can occur when the energies of the two states intersect, with the probability of a transition depending on an electronic coupling term. Three different mechanisms are considered for the transfer of an electron from the excited dimer (P*) to H. In one mechanism, an electron first moves from P to B, generating $P^+B^-$ as a transient intermediate state; the dynamics calculated for this pathway agree well with the kinetics measured experimentally. ($P^+H^-$ forms in 3–4 ps, with the concentration of the intermediate state remaining low throughout the reaction.) A mechanism in which an electron moves from B to H in the initial step also is possible, on the basis of the calculated free energies of the relevant charge-transfer states. A mechanism involving a mixing of P*, $P^+B^-$, and $P^+H^-$ by superexchange gives lower calculated rates but cannot be excluded. The effectiveness of all three mechanisms depends on a remarkable ability of the protein to stabilize the charge-transfer states but, at the same time, to keep the reorganization energies for the electron-transfer reactions small.

When the reaction center of a photosynthetic bacterium absorbs a photon, an electron is transferred from a bacteriochlorophyll dimer (P) to a molecule of bacteriopheophytin (H) in approximately 3 ps (Woodbury et al., 1985; Martin et al., 1986; Breton et al., 1986). The crystal structures of reaction centers from *Rhodopseudomonas viridis* and *Rhodobacter sphaeroides* have been solved to high resolution (Deisenhofer et al., 1986; Chang et al., 1986; Allen et al., 1987), and the electron-transfer steps that occur in the reaction center have been studied in some detail. [See Parson (1987) and Kirmaier and Holten (1987) for recent reviews.] The initial charge separation can be written as the radiationless process $P^*BH \rightarrow P^+BH^-$, where P* represents the lowest excited state of the reaction center and B is an additional molecule of bacteriochlorophyll that is located between P and H (Figure 1). Despite extensive kinetic studies (Kirmaier et al., 1985a,b; Woodbury et al., 1985; Paschenko et al., 1985; Martin et al., 1986; Breton et al., 1986; Wasielewski & Tiede, 1986; Shuvalov & Duysens, 1986) and theoretical work (Warshel, 1980; Friesner & Wertheimer, 1982; Parson et al., 1987; Fischer & Scherer, 1987; Marcus, 1987; Scherer & Fischer, 1987; Bixon et al., 1987; Michel-Beyerle et al., 1987; Warshel et al., 1988), the role of the monomeric bacteriochlorophyll B in the initial charge separation is not clear, and the detailed mechanism of the reaction is still unknown.

One possible mechanism for the photochemical reaction would be for an electron to hop first from the excited bacteriochlorophyll dimer to B, generating a charge-transfer state ($P^+B^-$) that decays quickly by the movement of an electron from $B^-$ to H. Because the intermediate state $P^+B^-$ cannot be resolved experimentally, the rate constant for the second step in this sequence would have to be greater than that for the first. A theoretical study based on the coordinates of the chromophores in the *Rp. viridis* reaction center indicated that the electronic coupling matrix elements for the two steps are consistent with the observed kinetics (Parson et al., 1987; Warshel et al., 1988). However, the energy of the intermediate state seemed likely to be too high to make this pathway energetically favorable. In order for energy to be conserved in the initial step, the energy of $P^+B^-$ would have to be similar to that of P*. A second possible mechanism, coupling of P* with $P^+H^-$ by superexchange with $P^+B^-$, also requires that the energy of $P^+B^-$ be close to that of P*. A third mechanism, the formation of $B^+H^-$ as an initial intermediate, appeared likely to be more favorable energetically but was calculated to have somewhat smaller coupling matrix elements (Parson et al., 1987; Warshel et al., 1988). In other recent theoretical analyses, Marcus (1987) has favored the pathway via $P^+B^-$,

† This work was supported by the Department of Energy and the National Science Foundation (Grants CHE-8519194 and DMB-8616153) and the NSF San Diego Supercomputer Center.

0006-2960/88/0427-0774$01.50/0 

Bixon et al. (1987) and Michel-Beyerle et al. (1987) have provided arguments supporting the superexchange mechanism, and Fischer and Scherer (1987) and Scherer and Fischer (1987) have pointed out attractive features of the mechanism involving $B^+H^-$.

Now that the structures are known for reaction centers from several different bacterial species, converting protein structural information into estimates of the rate of electron transfer has become a major challenge. A detailed examination of the structure is necessary in order to understand the role of the microscopic environment in controlling the charge separation process. The present paper utilizes the X-ray coordinates of the *Rb. sphaeroides* reaction center (Chang et al., 1986) for a preliminary exploration of the dynamics and energetics of the three possible reaction mechanisms. We show that, by starting with the crystal structure and using information on the reduction potentials of the electron carriers in solution, one can calculate the energies of the reaction center's charge-transfer states in a manner that is free of any adjustable parameters. The results indicate that the formation of $P^+B^-$ as an intermediate cannot be excluded on the basis of energetic considerations. The protein appears to solvate this charge-transfer state sufficiently strongly to move its energy close to that of $P^*$.

## Theoretical Approach

Our analysis of the primary charge separation process is based on the semiclassical trajectory approach described previously by Warshel (1976) and Warshel and Hwang (1986). In this approach, the probability that the system will be in a given electronic state ($i$) at time $t$ is obtained from

$$|a_i(t)|^2 = \sum_n \sum_j [P_{ji}(t_n)|a_j(t_n)|^2 - P_{ij}(t_n)|a_i(t_n)|^2] \quad (1a)$$

where the summations are over crossings of the energies of the various states of the system ($i,j$) and the $t_n$ are the times of such crossings. $P_{ij}(t_n)$ is the probability of a transition from state $i$ to state $j$ over the small time interval from $t_n - \delta$ to $t_n + \delta$ and is given by

$$P_{ij}(t_n) = (1/2\delta)\left|\int_{t_n-\delta}^{t_n+\delta}(-i/\hbar)H_{ij} \times \exp\left\{-(i/\hbar)\int_0^t(\epsilon_j - \epsilon_i)\,dt\right\}dt\right|^2_{\epsilon_i} \quad (1b)$$

where $H_{ij}$ is the Hamiltonian matrix element describing the interaction of states $i$ and $j$ and the $\epsilon$'s are the diabatic energies of the states. The time dependence of the energies is determined by propagating classical trajectories for the nuclear degrees of freedom (the coordinates of the protein and solvent). The subscript $\epsilon_i$ denotes evaluation of the energy gap $(\epsilon_j - \epsilon_i)$ with trajectories that are propagated over the potential in state $i$. The coupled equations (eq 1a) for the different $a_i$ are evaluated with the boundary condition that only state 1 is populated initially. The rapidly oscillating integrands in eq 1b contribute to $a_j$ only when fluctuations of the system lead to an intersection of $\epsilon_j$ and $\epsilon_i$. At the points where $\epsilon_j - \epsilon_i = 0$, there is a nonzero probability for electron transfer from state $i$ to state $j$, with the actual probability depending on $H_{ij}$. In a multidimensional system, the phases of the integrands become effectively randomized following a crossing of the trajectory from the reactant to the product state. Division of the trajectory into time intervals around intersections thus conveniently allows one to neglect interference effects. A justification of this procedure has been given by Warshel and Hwang (1986).

The seemingly oversimplified expresion for $P_{ij}$ in eq 1b appears to provide a rigorous tool for evaluating the dynamics of electron-transfer reactions. The time average of $P_{ij}$ gives a rate constant that converges (for systems that obey the linear-response approximation) to the standard Marcus (1965) expression in the high-temperature regime but with realistic microscopic parameters based on the actual dynamics of the system. In the low-temperature limit one can use a dispersed-polaron version of $P_{ij}$ to obtain the exact harmonic rate constant (Warshel & Hwang, 1986).

A calculation of the rate constant using eq 1a and 1b requires an evaluation of the relevant matrix elements and energies, $H_{ij}$ and $\epsilon_i$. The present work focuses on the control of the $\epsilon_i$ by the protein microenvironment and leaves the $H_{ij}$ as adjustable parameters. The reason for this is as follows. In contrast to the *Rp. viridis* structure, where we could evaluate the $H_{ij}$ by a configuration-interaction treatment (Parson & Warshel, 1987; Parson et al., 1987; Warshel et al., 1988), the separation between the $\pi$ atoms of P and B in the *Rb. sphaeroides* structure is outside the range of validity of well-calibrated semiempirical resonance integrals. (The distances between the closest $\pi$ atoms are $\sim$3.8 Å in *Rp. viridis* and $\sim$5.8 Å in *Rb. sphaeroides*.) To treat long-range interactions, one must find ways of calculating the effect of the intervening medium, which includes aromatic amino acid residues and the $\sigma$ atoms of the chromophores. A consistent calculation of this effect is a major challenge and will be addressed in a future work. However, this interesting question does not bear directly on the energetics of the charge-transfer states or on the time-dependent fluctuations of the energies that are the main subject of the present inquiry.

The diabatic energies $\epsilon_i$ are given by

$$\epsilon_i = V_P + V_{strain} + V^i_{QQ} + V^i_{P,R} + \alpha^{i,g} \quad (2)$$

Here $V_P$ is the force field of the protein–protein and water–protein interactions. $V_{strain}$ is the intramolecular force field of the reacting bacteriochlorophyll and bacteriopheophytin molecules in the ground state without the (vacuum) intermolecular electrostatic interactions, which are represented by $V^i_{QQ}$. $V^i_{P,R}$ represents the interaction of the atoms of the bacteriochlorophyll and bacteriopheophytin molecules with the rest of the protein–water system, including the effects of the protein residual charges, nearby water molecules, and the induced dipoles in the protein. The $\alpha^{i,g}$ are the differences between the gas-phase free energies of the indicated states and the ground state, at infinite separation between the oxidized and reduced fragments.

To evaluate $V_p$, $V_{strain}$, and $V^i_{P,R}$, we used the classical force fields described by Warshel and Levitt (1976). Interactions of the protein and the chromophores with water, and the interactions among the water molecules themselves, were treated as described by Warshel and Russell (1984) and Warshel et al. (1986). The atomic charges needed to evaluate $V^i_{QQ}$ and $V^i_{P,R}$ were obtained by the QCFF/PI (quantum mechanical consistent force field/$\pi$ electrons) method (Warshel, 1977; Warshel & Lapicirella, 1981; Warshel & Parson, 1987). Induced dipoles in the protein were evaluated (in kcal/mol) as

$$V_{ind} = -166\sum_k \gamma_k(\xi^0_k)^2/d \quad (3)$$

where $\xi^0_k$ is the vacuum field (in atomic charges/Å$^2$) on the $k$th protein atom from the charges and residual charges of the system, $\gamma_k$ are the atomic polarizabilities (in Å$^3$), and $d$ is an effective screening function (Russell & Warshel, 1985). The screening function in this equation has been parametrized in

previous studies (Russell & Warshel, 1985) and is not to be confused with the dielectric constant. Because of compensating effects of the induced dipoles, the calculated electrostatic energies are relatively insensitive to the exact set of residual charges that are used to represent the permanent dipoles in the protein [see Figure 8 of Russell and Warshel (1985)]. Similar values for $V_P$ and $V^i_{P,R}$ should be obtained with any of the other molecular dynamics programs that are currently available, provided that the program is modified to include induced dipoles.

Induced dipoles in the protein play a particularly important role in stabilizing the nonequilibrium charge-transfer states (Warshel & Russell, 1984). The effect of protein polarizability cannot be estimated reliably by unscaled macroscopic approaches, and little direct experimental information is available on this point. [Michel-Beyerle et al. (1987) recently have attempted to assess ionization energies in the reaction center on the basis of experimental work by Nakato et al. (1977). However, Nakato et al. actually give only theoretical estimates based on the Born formula, which depends on an unknown cavity radius.]

The force field involving the protein alone or the interactions of the protein with the solvent, $V_P$, is independent of the redox state of the electron carriers. Although $V_{strain}$ is expected to vary somewhat among the different states, we take it to be identical for all of the states considered here. This neglects changes in the intramolecular equilibrium geometries of the chromophores upon transitions between different states; the differences in the equilibrium energy values are included in the corresponding $\alpha^g$'s. Previous QCFF/PI calculations have shown that correction terms for this simplification are relatively small (Warshel, 1980). Neglecting the changes in equilibrium geometry is equivalent to treating the intramolecular motion quantum mechanically by the approach described in Warshel and Hwang (1986) but considering only the $0 \rightarrow 0$ vibronic transition. For the backreactions, which are not treated here, one will have to consider the $0 \rightarrow n$ transitions.

With this simplification of $V_{strain}$, the difference between the energy of state $i$ and that of the ground state at any point during the trajectory is

$$\Delta\epsilon_i = \Delta(V^i_{P,R} + V^i_{QQ}) + \alpha^{i,g} \quad (4a)$$

The corresponding free energy difference between state $i$ and the ground state is

$$\Delta G^i = \Delta G^i_{elec} + \alpha^{i,g} \quad (4b)$$

where $\Delta G^i_{elec}$ is the change in electrostatic free energy associated with $V^i_{P,R} + V^i_{QQ}$ for the formation of the given state.

The free energy change for the formation of a charge-transfer state can be calculated most reliably by a free energy perturbation method, in which one essentially carries out an adiabatic "charging" of the electron carriers:

$$\Delta G^i = \sum \delta G(\theta_m \rightarrow \theta_{m'}) \quad (5a)$$

$$\delta G(\theta_m \rightarrow \theta_{m'}) = -(k_B T) \ln \{\langle \exp(-[\epsilon_{m'} - \epsilon_m]/k_B T)\rangle_{\epsilon_m}\} \quad (5b)$$

$$\epsilon_m = \theta_m \epsilon_i - (1 - \theta_m)\epsilon_0 \quad (5c)$$

Here $k_B$ is the Boltzmann constant and $\theta_m$ and $\theta_{m'}$ are successive values of the mapping parameter $\theta$, which increases gradually from 0 to 1. This method has been used successfully in other recent studies (Warshel et al., 1986; Singh et al., 1987).

To find the gas-phase energy differences for the formation of the charge-transfer states, $\alpha^{i,g}$, we followed an approach that has been used previously for studying electrostatic energies in proteins (Warshel & Russell, 1984). The key idea is to take as reference states the corresponding states when the electron carriers are separated to an infinite distance in a polar solvent. The free energy change for the electron-transfer reaction that forms such a reference state is

$$\Delta G^{i,W}(\infty) = \Delta I^W_{i^+} + \Delta I^W_{i^-} = \alpha^{i,g} + \Delta G^{i,W}_{sol}(\infty) \quad (6)$$

Here $\Delta I^W_{i^+}$ and $\Delta I^W_{i^-}$ are the free energy changes associated with forming the charged $i^+$ and $i^-$ fragments independently in solution. These free energies can be obtained experimentally from the standard redox potentials of the two half-reactions. $\Delta G^{i,W}_{sol}(\infty)$ is the total solvation free energy for the oxidized and reduced species at infinite separation, relative to the solvation free energy of the uncharged species. The solvation free energies of the individual components, $\Delta G^W_{i^+,sol}(\infty)$ and $\Delta G^W_{i^-,sol}(\infty)$, can be calculated by the free energy perturbation method described above (eq 5a–c). Thus the solvation free energies provide a way of getting the energies of the fragments from *experimental* redox potentials, avoiding unreliable quantum mechanical calculations of the gas-phase energies of the large chromophores.

Note that the time average of the energy difference in eq 1b, $\langle \epsilon_j - \epsilon_i \rangle_{\epsilon_i}$, generally differs from $\langle \epsilon_j \rangle_{\epsilon_j} - \langle \epsilon_i \rangle_{\epsilon_i}$ because the averages of $\epsilon_j$ involve the force fields in two different states. The difference between the two averages is related to the solvent (protein) reorganization energy $\lambda_{ij}$ (Hwang & Warshel, 1987):

$$\lambda_{ij} = \langle \epsilon_j - \epsilon_i \rangle_{\epsilon_i} - (\Delta G^j - \Delta G^i) \quad (7)$$

In order for $\langle \epsilon_j - \epsilon_i \rangle_{\epsilon_i}$ to be close to zero so that the reaction will be activationless, as electron transfer from P to H is found to be (Woodbury et al., 1985; J.-L. Martin and J. Breton, personal communication), $\lambda_{ij}$ must be approximately equal to $(\Delta G^i - \Delta G^j)$.

For $P^*$, $\Delta G^i$ can be equated with the experimentally measured 0–0 transition energy of the reaction center's long-wavelength absorption band. The solvation energy of P* depends on the admixture of charge-transfer transitions and local transitions that make up the excited state (Parson & Warshel, 1987) and cannot yet be calculated unambiguously. On the basis of the calculated change in dipole moment associated with the formation of P*, we estimate the solvation energy to be approximately −1 kcal/mol, but this number does not enter into any of our subsequent calculations.

The reaction center was modeled by using the coordinates for the chromophores and protein of *Rb. sphaeroides* (Chang et al., 1986). The crystal structure has been refined to a resolution of 3.1 Å with $R = 0.26$. Our calculations include all six chromophores and all of the amino acids that have one or more atoms within 14 Å of a point halfway between the centers of P and B (or between P and H, depending on the state under consideration). This amounts to approximately 4500 atoms. [Including the entire amino acid residues ensures electrical neutrality (Warshel et al., 1986).] Water molecules were allowed to fill all of the cavities within this region. This procedure (Russell & Warshel, 1985) allows one to include loosely bound waters, which generally are not visible in an X-ray structure until the resolution is better than about 2 Å. The microscopic system was completed to a sphere by adding a cubic grid of induced dipoles with a spacing of 2 Å and a polarizability of 1 Å$^3$ (Warshel & Russell, 1984). The region outside this sphere was modeled as a continuum with a dielectric constant of 2. This is an approximation of the response of the membrane or detergent surrounding the reaction center to the weak field from a charge at a large distance; it does not imply that the protein itself has a dielectric constant of 2. The

glutamic acid residue that probably forms a hydrogen bond to the keto group of H (E104 of the L subunit) was assumed to be in the form of the un-ionized acid.

Room for approximately five water molecules was found inside a shell of 4.5 Å around P and B. In general, the neglect of solvation by water can cause significant errors in the self-energies of ions, leading to incorrect conclusions about the microscopic screening of charge–charge interactions (Russell & Warshel, 1985). However, the calculated energies are not sensitive to the exact positioning of the water molecules, which are free to move during the simulation. In the present case, induced dipoles in the protein are probably more important than bound water, because of the large sizes of the charged species and the relatively nonpolar nature of the protein. The contribution of water to the calculated free energy of $P^+B^-$ was approximately −3 kcal/mol, compared to a contribution of approximately −16 kcal/mol from induced dipoles.

A correct treatment of the intermolecular potential surface for the two bacteriochlorophylls of P requires one to use Löwdin overlap corrections within the QCFF/PI potential (Warshel, 1980). Here we used a simplified treatment with the same standard van der Waals interactions that were used for the atoms of the protein and the classical interatomic electrostatic interactions. In addition, we applied a quadratic constraint that maintained the average center-to-center intermolecular distance given by the X-ray coordinates. This approximation probably does not introduce any major errors, because previous calculations that included the Löwdin correction have indicated that the intradimer reorganization energy is relatively small (Warshel, 1980). In $P^+$, the positive charge was divided equally between the two bacteriochlorophylls of the special pair ($P_M$ and $P_L$). We also examined a more rigorous model in which $P^+B^-$ was treated as a superposition of two interacting states, $P_M{}^+B^-$ and $P_L{}^+B^-$. This gave very similar electrostatic energies (within ±1 kcal/mol), probably because $P_M$ and $P_L$ are nearly equidistant from B.

Equilibration of the calculated structure was achieved by keeping the average kinetic energy low initially so that the temperature did not exceed 30 K and then increasing the temperature gradually to the desired region. Following the equilibration period, the results of the free energy perturbation calculations were independent (within ±1 kcal/mol) of whether a time interval of 2 or 3 ps was used for each increment in $\theta$; we routinely used the longer interval. Forward and backward charging ($P \rightarrow P^+B^-$) and discharging ($P^+B^- \rightarrow P$) cycles also were shown to give the same results within ±1 kcal/mol. However, these tests check only for convergence. The possible errors in the calculated energies are larger than ±1 kcal/mol, primarily because of uncertainties in the positions of the chromophores. Uncertainties in the crystal structure could bear on almost all of the parameters that enter into the calculations, including the amount of space that is available to accomodate water. To examine the possible effects of errors in the structure, we perturbed the positions of the chromophores and the surrounding protein by introducing a quadratic constraint between the centers of $P^+$ and $B^-$. Changing the center-to-center distance by 1 Å resulted in a change of 5 kcal/mol in the calculated value of $\Delta G$ for $P^+B^-$. This is probably an upper limit for the uncertainties in the values of $\Delta G^i$ listed in Table I. Movements of the chromophores have smaller effects on the calculated reorganization energies, $\lambda_{ij}$; the uncertainties in these values are probably less than ±2 kcal/mol.

Considering the complexity of the problem, it may seem surprising that one can calculate the free energies of

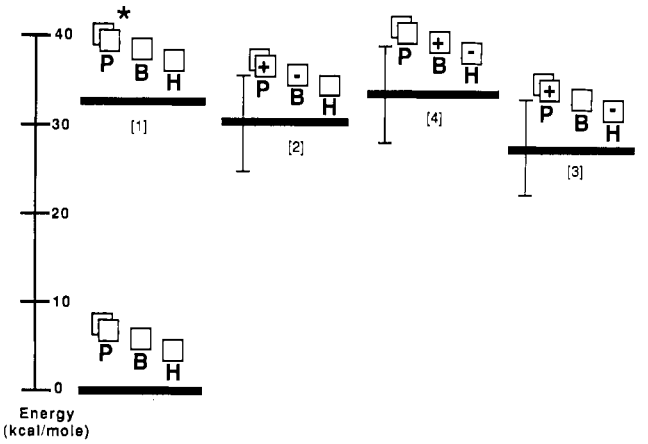


FIGURE 1: Diabatic states that could contribute to the primary charge-separation process in the bacterial reaction center. The zero of the free energy scale is for the ground electronic state with the protein relaxed to the corresponding equilibrium geometry. For states 2, 3, and 4, the error bars bracket our estimates of the free energies, based on calculations using free energy perturbation methods and experimental redox potentials. See the text and Table I for details.

charge-transfer states in the reaction center with an uncertainty as small as ±5 kcal/mol. Because of the enormous dimensionality of the protein, it is not possible to establish a rigorous error range; this would require one to run an infinitely long trajectory. However, an error range of ±5 kcal/mol is not out of line with the results of other recent studies in which the calculated free energies could be checked experimentally. For example, in the closely related case of electron transfer between cytochrome *c* and the octapeptide–heme complex obtained by hydrolysis of the cytochrome, the calculated and measured free energies differed by only 2 kcal/mol (Churg & Warshel, 1986). The treatment of the solvent in those calculations was based in part on the PDLD (protein dipole Langevin dipole) method, which is less accurate than the free energy perturbation method that we have used here. Similar agreement between calculated and measured free energies was obtained in a study of ion-pair energetics in trypsin [see Figure 23 of Warshel and Russell (1984)]. Even more accurate values have been obtained by several groups who have used the free energy perturbation method to calculate solvation energies in solutions (Warshel et al., 1986; Singh et al., 1987) and in proteins (Warshel et al., 1986; Wong & McCammon, 1986). In some of these cases, the calculated and experimental energies differ by less than 1 kcal/mol. Reliable predictions of the energies of charged transition states in enzymatic catalysis also have been reported (Hwang & Warshel, 1987; Rao et al., 1987). In the present case, the uncertainties in the protein structure contribute additional sources of error, because the chromophore–chromophore distances and the cavities available for water are likely to change somewhat with further refinement of the structure.

## Results and Discussion

The diabatic electronic states of interest are shown schematically in Figure 1. To consider the "hopping" and superexchange mechanisms involving $P^+B^-$, we take state 1 to be the lowest excited singlet state of the reaction center (P*), state 2 to be the $P^+B^-$ charge-transfer state, and state 3 to be $P^+H^-$. For the alternative "hole-transfer" mechanism, we label $B^+H^-$ as state 4.

Table I summarizes the free energy perturbation calculations. By combining the experimental standard redox potentials of the electron carriers with the calculated solvation free energies for the individual oxidants and reductants, one can

Table I: Diabatic Energies of Fragments and States[a]

| | fragments | | | |
|---|---|---|---|---|
| | $B^-$ | $B^+$ | $P^+$ | $H^-$ |
| $E_m$ | −0.86 | +0.64 | +0.45[b] | −0.55 |
| $\Delta I_{i\pm}^W$ | 19.8 | 14.8 | 10.4[b] | 12.8 |
| $\Delta G_{i\pm,sol}^W(\infty)$ | −30 | −30 | −24[b] | −30 |

| | states | | | | |
|---|---|---|---|---|---|
| | $P^0$ (0) | $P^*$ (1) | $P^+B^-$ (2) | $P^+H^-$ (3) | $B^+H^-$ (4) |
| $\Delta G^{i,W}(\infty)$ | | | 30 | 23 | 28 |
| $\Delta G_{sol}^{i,W}(\infty)$ | 0 | −1 | −55 | −55 | −60 |
| $\alpha^{i,g}$ | 0 | 33 | 85 | 78 | 88 |
| $\Delta G_{elec}^i$ | 0 | −1 | −55 | −50 | −55 |
| $\Delta G^i$ | 0 | 32[c] | 30 | 28 | 33 |
| $\lambda_{ij}$ | | | 4 (1 → 2) | 5 (1 → 3) | |
| | | | | 5 (2 → 3) | |

[a] All values are in kcal/mol except for the standard redox potentials ($E_m$), which are in V. $E_m$ and $\Delta I^W$ are given relative to the hydrogen electrode at pH 0. The estimated uncertainties in the $\alpha^{i,g}$ and $\Delta G^i$ are ±5 kcal/mol; those in the $\lambda_{ij}$ are ±2 kcal/mol. [b] The measured redox potential of $P/P^+$ and the calculated solvation free energy of $P^+$ are for the bacteriochlorophyll dimer in the protein. The solvation energy calculated for a dimer with the same structure in aqueous solution is −25 kcal/mol. [c] Observed value.

estimate the $\alpha^{i,g}$, which are needed in order to obtain the energies of the various states in the protein. Redox potentials for the oxidation and reduction of monomeric bacteriochlorophyll and bacteriopheophytin in organic solvents containing electrolytes have been measured by Fajer et al. (1976). The redox potentials can be converted straightforwardly into the free energy changes for forming the oxidized or reduced electron carriers in solution, relative to the standard hydrogen half-cell reaction. Solvation energies of $B^-$, $H^-$, and $B^+$ were calculated for aqueous solution as outlined above. Although it would be desirable for the calculations to model the same solvent that was used for the redox measurements, previous studies have shown that solvation energies for ions in polar organic solvents are approximately the same as those for aqueous solution, to within about ±2 kcal/mol (Warshel & Russell, 1984). For the bacteriochlorophyll dimer P, the experimentally measured redox potential of +0.45 V (Dutton & Jackson, 1972) includes the effects of "solvation" by the protein, in addition to bound water and the surrounding solution. The solvation free energy associated with the formation of $P^+$ in the reaction center was calculated to be −24 kcal/mol (Table I). For comparison, the solvation free energy for the oxidation of a bacteriochlorophyll dimer with the same structure in water was calculated to be −25 kcal/mol. The stabilization of $P^+$ by the protein thus appears to be very close to the stabilization that would be possible in solution.

Figure 2A shows the time-dependent energy gap between $P^*$ (state 1) and $P^+B^-$ (state 2) for a trajectory on state 1 at 100 K. By evaluating eq 1a and 1b over this trajectory, one can obtain the time dependence of transitions from state 1 to state 2. Transitions from state 2 to state 3 can be evaluated similarly by following trajectories on state 2. This allows one to model the hopping mechanism, in which $P^+B^-$ is a discrete intermediate. To treat the second step properly, the second trajectory should begin immediately after the formation of $P^+B^-$, before the system has relaxed toward the equilibrium configuration of this state. The results then should be averaged over many different trajectories for each of the two transitions. For the present initial study, we have used the curve shown in Figure 2A to model the energy fluctuations for both transitions. However, the mean levels for the energy gaps in the two steps were adjusted to be in accord with the values of $\alpha^{2,g}$ and $\alpha^{3,g}$ and the reorganization energies given in Table I.

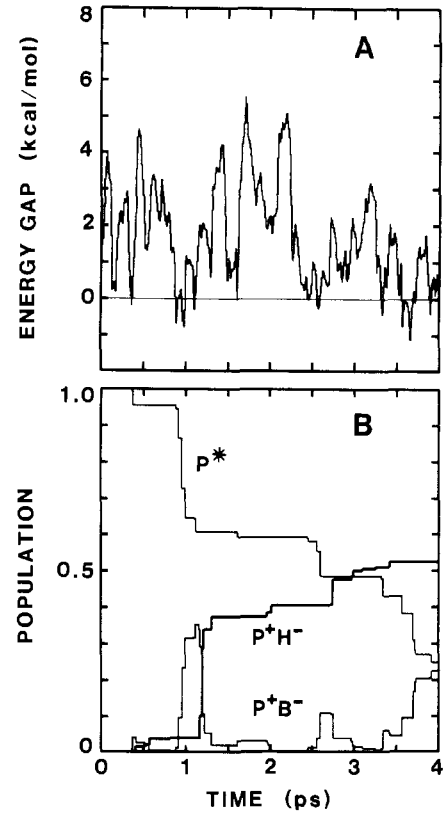


FIGURE 2: (A) Energy gap between state 2 ($P^+B^-$) and state 1 ($P^*$) and as a function of time for a trajectory propagated on the potential energy surface of state 1. The energy gap provides a direct way of simulating the kinetics of electron transfer (eq 1). The trajectory shown here was calculated for a temperature of 100 K, following an equilibration period of approximately 10 ps. (B) Calculated populations ($|a_i|^2$) of states 1, 2, and 3 as a function of time with the hopping model. Coupling matrix elements: $H_{12}$ = 10 $cm^{-1}$ and $H_{23}$ = 25 $cm^{-1}$. The average energy of state 2 was taken to be 600 $cm^{-1}$ (1.7 kcal/mol) above that of state 1 (see panel A); state 3 was put 100 $cm^{-1}$ (0.3 kcal/mol) below state 2. Note that the energy gap for each step of the pathway refers to a trajectory on the potential energy surface of the reactant state for that step, not to the difference between the equilibrium free energies of the reactant and product. The average energy gaps used for this simulation are approximately the values obtained by adding the calculated $\lambda_{ij}$ (Table I) to the calculated values of ($\Delta G^j - \Delta G^i$).

Figure 2B shows the overall kinetics that are predicted for the hopping sequence by using the energy fluctuations from Figure 2A and taking $H_{12}$ as 10 $cm^{-1}$ and $H_{23}$ as 25 $cm^{-1}$. As was noted above, we have treated the matrix elements as free parameters and have adjusted them so that the overall reaction occurs on the time scale of approximately 3 ps, in agreement with the experimental observations. The values chosen are within a factor of 2 of the matrix elements of 6 $cm^{-1}$ for $H_{12}$ and 15 $cm^{-1}$ for $H_{23}$ that were calculated for *Rp. viridis* (Parson et al., 1987; Warshel et al., 1988).

To approximate the effect of averaging the calculations over many different trajectories, one can average the results of starting the calculations at many randomly chosen points on a single trajectory. This procedure will be rigorous if the trajectory is long enough so that its autocorrelation function converges. Figure 3A shows such an average. The results successfully reproduce the main features of the observed reaction kinetics: $P^+H^-$ is formed in 3–4 ps, with a marginally detectable amount of the intermediate $P^+B^-$ state. In more refined calculations that are currently in progress, we have used three independent waveforms for the energy gaps between states 1 and 2, 2 and 3, and 1 and 3; the results are very similar to those shown in Figure 3A. These calculations will be re-

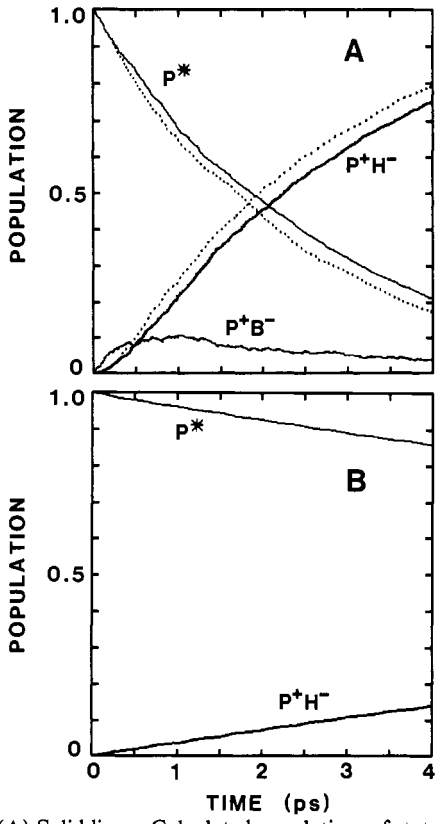


FIGURE 3: (A) Solid lines: Calculated populations of states 1, 2, and 3 as a function of time with the hopping model as in Figure 2B but for an average of 100 simulations with the fluctuations in each of the two energy gaps started at random times along the trajectory. Other conditions as in Figure 2. Dotted lines: Calculated populations when superexchange is added to hopping. For the superexchange pathway, the average energy of state 3 was taken to be 300 $cm^{-1}$ (0.8 kcal/mol) above that of state 1, and the fluctuations in this energy gap were started at random times relative to those in the other two gaps; other conditions were as for the solid lines. The matrix element connecting states 1 and 3 by superexchange depends on $H_{12}$ and $H_{23}$ and on the energy gaps between the states and was evaluated at each step in the trajectory. (B) Calculated populations of states 1 and 3 for the superexchange mechanism when the average energy gap between states 1 and 2 is increased to 1600 $cm^{-1}$ (4.6 kcal/mol). This energy gap is near the upper bound of our error range (Table I). $H_{12}$ was increased to 35 $cm^{-1}$ and $H_{23}$ to 80 $cm^{-1}$. The mean energy gaps between states 1 and 3 and between states 2 and 3 were left at 300 and −100 $cm^{-1}$, respectively, as in Figure 3A. The increase in the energy gap between states 1 and 2 prevents hopping between these two states. A total of 100 simulations were averaged, with the fluctuations in each of the three energy gaps starting at random times on the trajectory.

ported in detail subsequently, along with the results of calculations for other temperatures.

The most important conclusion to be drawn from Figures 2 and 3 is that the hopping mechanism is feasible, due to a favorable electrostatic control by the protein. The average time-dependent energy gap between $P^+B^-$ and P* evidently is smaller in the protein than it would be in water. To accomplish this, the protein must stabilize the $P^+B^-$ charge-transfer state nearly as well as water could but at the same time make the reorganization energy for the charge-transfer process ($\lambda_{12}$) less than it would be in water. The calculated reorganization energy for the formation of $P^+B^-$ in the protein is only 4 kcal/mol (Table I), whereas the reorganization energy in water is approximately 30 kcal/mol. Similarly, the protein appears to have a surprisingly small reorganization energy of about 5 kcal/mol for the formation of $P^+H^-$, while the corresponding electrostatic free energy of $P^+H^-$ is only about 5 kcal/mol larger than the calculated free energy for this species in water.

For a protein to provide both a large effective solvation energy and a small reorganization energy for an ion pair with ions having such a large radius is not at all trivial. In general, when the charge centers are far apart, the solvation by a protein is similar to that provided by water, but the corresponding reorganization energy also is large (Warshel & Russell, 1984). In the related case of cytochrome *c*, the reorganization energy is smaller than the reorganization energy calculated for water, but the heme is held in a low-dielectric environment, and its solvation is about 7 kcal *less* than that in water. The trick used by the reaction center could be associated with the bacteriochlorophyll dimer. $P^+$ presents a very delocalized charge, which is associated with a relatively small solvation energy (Table I) and a moderate oxidation potential. Since $\Delta G_{sol}$ is small for both $P^+B^-$ and $P^+H^-$ (the surrounding medium is not polarized strongly by these states), it is possible for the protein's permanent and induced dipoles to provide nearly as much solvation as water does and at the same time to have a smaller reorganization energy than the corresponding system in solution.

It is notable in this regard that the fluctuations in $\Delta\epsilon$ shown in Figure 2A are much smaller than the fluctuations that have been obtained in studies of enzyme active sites, where there generally are more concentrated local charges (Warshel & Russell, 1984). The relaxations associated with changes in the charging parameter $\theta$ also are smaller than the relaxations that have been calculated in previous studies of enzymes and solutions. These interesting findings will require more detailed study before their structural basis will be clear.

If $\alpha^{2,g}$ is increased from 85 to 88 kcal/mol, the upper limit of the estimate given in Table I, intersections of the energies of states 1 and 2 are effectively prevented, and the hopping model is no longer able to simulate the observed kinetics no matter how large one makes the matrix elements $H_{12}$ and $H_{23}$. Under these conditions, superexchange could become the dominant mechanism of charge separation. In the superexchange mechanism, one considers the initial state to be a quantum mechanical mixture of states 1 and 2 and expresses the coupling to $P^+B^-$ (state 3) in terms of the coefficient of state 2 in the mixture (Warshel et al., 1988). During a trajectory on state 1, the coefficient fluctuates as a function of the energy gap between states 1 and 2. Transitions to state 3 can occur when there is an intersection of the energies of states 1 and 3. Under the conditions used for Figures 2 and 3A, superexchange is less effective than the formation of $P^+B^-$ as an actual intermediate. As shown by the *dotted lines* in Figure 3A, including superexchange in the calculation in addition to hopping increases the overall rate of the reaction by only about 10%. If $\alpha^{2,g}$ is increased so that hopping is prevented and the matrix elements $H_{12}$ and $H_{23}$ are left at the values used for Figure 3A (10 and 25 $cm^{-1}$, respectively), the calculated rate of electron transfer by superexchange is far below the rate found experimentally. However if $H_{12}$ and $H_{23}$ are increased to 35 and 80 $cm^{-1}$, one obtains a small but significant reaction by superexchange (Figure 3B). Thus, the superexchange mechanism seems unfavorable but cannot be excluded by the present study, considering the uncertainties in the matrix elements and the energies. Note that in order to obtain an activationless rate by superexchange, it is necessary for state 3 to intersect frequently with state 1. The calculations do place the unrelaxed state 3 at an optimal position for superexchange, with a $\lambda_{13}$ of 5 kcal/mol (Table I).

The "hole-transfer" mechanism, in which an electron first moves from B to H to generate $B^+H^-$ as a transient inter-

mediate, was not simulated in detail. On the basis of the values of $\Delta G$ and $\lambda$, this mechanism appears to be somewhat less favorable than the channel via $P^+B^-$, because the energy of the relaxed $B^+H^-$ is calculated to be above that of $P^+B^-$ (Table I). However, calculations based on a more refined structure will be needed for a detailed comparison of the two pathways.

Although the present study is only a preliminary exploration, it is encouraging that the uncertainty in the calculated energies is no greater than 5 kcal/mol. Attempting to perform such calculations without considering the induced dipoles in the protein, without including loosely bound water molecules, or by using calculated gas-phase ionization energies rather than redox cycles of the type that we have used here could lead to built-in errors of 20 kcal/mol or more. One indication of the reliability of our aproach is that the calculated free energy of $P^+H^-$ ($28 \pm 5$ kcal/mol, Table I) agrees satisfactorily with experimental estimates of 28 kcal/mol at 295 K and 30 kcal/mol at 100 K (Woodbury & Parson, 1984). [These experimental free energies are for an "initial" form of $P^+H^-$, as examined on a time scale of about 1 ns. Hörber et al. (1986) and Boxer et al. (1988) have obtained values between 26 and 27 kcal/mol, which also fall within our error range but may pertain to a more relaxed state of the reaction center.] It is important to note that the calculated free energies presented here, as well as all of the reorganization energies, were obtained without using any adjustable parameters or an arbitrary dielectric constant.

The type of microscopic simulation described here has several advantages over other possible approaches to calculating the energies of charge-transfer states in proteins. Yeates et al. (1987) recently have used a macroscopic discrete-continuum model to examine the energetics of placing a negative charge on B or H. Such calculations do not address the actual charge-separation process that forms the $P^+B^-$ or $P^+H^-$ ion pair but rather the process of bringing a single charge in from an infinite distance. Moreover, the macroscopic model depends strongly on the value chosen for the dielectric constant of the protein, and this number is subject to considerable uncertainty. Michel-Beyerle et al. (1987) have used a dielectic constant of 2 for evaluating charge–charge interactions in the $P^+H^-$ charge-transfer state, whereas much larger values typically are found in proteins (Warshel & Russell, 1984). Changing the protein's dielectric constant from 2 to 20 would result in a 30 kcal/mol change in the interaction energy of two charges 5 Å apart. In addition, the macroscopic Born formula that Michel-Beyerle et al. (1987) have used to estimate the polarization energy of $P^+H^-$ includes a cavity radius as an adjustable parameter. Thus it appears to us that the only way to deal realistically with the complicated environment in a protein such as the reaction center is by an explicit microscopic simulation.

It will be interesting to compare the results obtained here with similar calculations on the *Rp. viridis* reaction center when the protein coordinates for that species become available. An additional test of our approach will be to calculate the free energy of the radical pairs $P^+Q_A^-$ and $P^+Q_B^-$, in which an electron is transferred from P to one of the two quinones in the reaction center ($Q_A$ and $Q_B$). These free energies have been measured experimentally by several different techniques. The approach also can be tested by calculations on genetically modified reaction centers with altered amino acids in the vicinity of the chromophores.

ACKNOWLEDGMENTS

We thank Drs. M. Schiffer and C. Chang for providing the X-ray coordinates of the reaction center and Drs. S. Boxer, J. Breton, S. Fischer, R. Marcus, and M. E. Michel-Beyerle for informing us of some of their recent results prior to publication.

REFERENCES

Allen, J. P., Feher, G., Yeates, T. O., Komiya, H., & Rees, D. C. (1987) *Proc. Natl. Acad. Sci. U.S.A. 84*, 5730–5734.

Bixon, M., Jortner, J., Michel-Beyerle, M. E., Ogrodnik, A., & Lersch, W. (1987) *Chem. Phys. Lett. 140*, 626–630.

Boxer, S. G., Goldstein, R. A., Lockhart, D. J., Middendorf, T. R., & Takiff, L. (1988) *Structure of Bacterial Reaction Centers—X-ray Crystallography and Optical Spectroscopy with Polarized Light* (Berton, J., & Vermeglio, A., Eds.) Plenum, New York (in press).

Breton, J., Martin, J.-L., Hoff, A., Migus, A., Antonetti, A., & Orsag, A. (1986) *Proc. Natl. Acad. Sci. U.S.A. 83*, 5121–5125.

Chang, C.-H., Tiede, D., Tang, J., Smith, U., Norris, J., & Schiffer, M. (1986) *FEBS Lett. 205*, 82–86.

Churg, A., & Warshel, A. (1986) *Biochemistry 25*, 1675–1681.

Deisenhofer, J., Epp, O., Miki, K., Huber, R., & Michel, H. (1985) *Nature (London) 318*, 618–624.

Dutton, P. L., & Jackson, J. B. (1972) *Eur. J. Biochem. 30*, 63–80.

Fajer, J., Davis, M. S., Brune, D. C., Spaulding, L. D., Borg, D. C., & Forman, A. (1976) *Brookhaven Symp. Biol. 28*, 74–103.

Fischer, S. F., & Scherer, P. O. J. (1987) *Chem. Phys. 115*, 151–158.

Friesner, R., & Wertheimer, R. (1982) *Proc. Natl. Acad. Sci. U.S.A. 79*, 2138–2142.

Hörber, J. K. H., Göbel, W., Ogrodnik, A., Michel-Beyerle, M. E., & Cogdell, R. J. (1986) *FEBS Lett. 198*, 273–278.

Hwang, J.-K., & Warshel, A. (1987) *J. Am. Chem. Soc. 109*, 715–720.

Kirmaier, C., & Holten, D. (1987) *Photosynth. Res. 13*, 225–260.

Kirmaier, C., Holten, D., & Parson, W. W. (1985a) *Biochim. Biophys. Acta 810*, 33–48.

Kirmaier, C., Holten, D., & Parson, W. W. (1985b) *FEBS Lett. 185*, 76–82.

Marcus, R. (1965) *J. Chem. Phys. 43*, 679–701.

Marcus, R. (1987) *Chem. Phys. Lett. 133*, 471–477.

Martin, J.-L., Breton, J., Hoff, A., Migus, A., & Antonetti, A. (1986) *Proc. Natl. Acad. Sci. U.S.A. 83*, 957–961.

Michel-Beyerle, M. E., Plato, M., Deisenhofer, J., Michel, H., Bixon, M., & Jortner, J. (1987) *J. Chem. Phys.* (in press).

Nakato, Y., Koichi, A., & Tsubomura, H. (1976) *Chem. Phys. Lett. 39*, 358–360.

Parson, W. W. (1987) in *Photosynthesis* (Amesz, J., Ed.) pp 43–61, Elsevier, Amsterdam.

Parson, W. W., & Warshel, A. (1987) *J. Am. Chem. Soc. 109*, 6152–6163.

Parson, W. W., Creighton, S., & Warshel, A. (1987) in *Primary Processes in Photobiology* (Kobayashi, T., Ed.) pp 43–51, Springer-Verlag, Berlin.

Paschenko, V. Z., Korvatovskii, B. N., Kononenko, A. A., Chamorovsky, S. K., & Rubin, A. B. (1985) *FEBS Lett. 191*, 245–248.

Rao, S. N., Singh, U. C., Bash, P. A., & Kollman, P. A. (1987) *Nature (London) 328*, 551.

Russell, S., & Warshel, A. (1985) *J. Mol. Biol. 185*, 389–404.

Scherer, P. O. J., & Fischer, S. F. (1987) *Chem. Phys. Lett. 141*, 179.

Shuvalov, V. A., & Duysens, L. N. M. (1986) *Proc. Natl. Acad. Sci. U.S.A. 83*, 1690-1694.
Singh, U. C., Brown, F. K., Bash, P. A., & Kollman, P. A. (1987) *J. Am. Chem. Soc. 109*, 1607-1614.
Warshel, A. (1976) *Nature (London) 260*, 679-683.
Warshel, A. (1977) in *Modern Theoretical Chemistry* (Segal, G., Ed.) Vol. 7, pp 133-172, Plenum, New York.
Warshel, A. (1980) *Proc. Natl. Acad. Sci. U.S.A. 77*, 3105-3109.
Warshel, A., & Levitt, M. (1976) *J. Mol. Biol. 103*, 227-249.
Warshel, A., & Lapicirella, A. (1981) *J. Am. Chem. Soc. 103*, 4664-4673.
Warshel, A., & Russell, S. (1984) *Q. Rev. Biophys. 17*, 283-422.
Warshel, A., & Hwang, J.-K. (1986) *J. Chem. Phys. 84*, 4938-4957.
Warshel, A., & Parson, W. W. (1987) *J. Am. Chem. Soc. 109*, 6143-6152.
Warshel, A., Sussman, F., & King, G. (1986) *Biochemistry 25*, 8368-8372.
Warshel, A., Creighton, S., & Parson, W. W. (1988) *J. Phys. Chem.* (in press).
Wasielewski, M. R., & Tiede, D. M. (1986) *FEBS Lett. 204*, 386-372.
Wong, C. F., & McCammon, A. (1986) *J. Am. Chem. Soc. 108*, 3830-3832.
Woodbury, N. W., & Parson, W. W. (1984) *Biochim. Biophys. Acta 767*, 345-361.
Woodbury, N. W., Becker, M., Middendorf, D., & Parson, W. W. (1985) *Biochemistry 24*, 7516-7521.
Yeates, T. O., Komiya, H., Rees, D. C., Allen, J. P., & Feher, G. (1987) *Proc. Natl. Acad. Sci. U.S.A. 84*, 6438-6442.

# Nucleotide Binding to Uncoupling Protein. Mechanism of Control by Protonation†

Martin Klingenberg
*Institut für Physikalische Biochemie der Universität München, Goethestrasse 33, 8000 München 2, FRG*
*Received February 18, 1987; Revised Manuscript Received September 17, 1987*

ABSTRACT: Nucleotide binding to the isolated uncoupling protein (UCP) from brown adipose tissue of hamster was studied in detail under equilibrium conditions. Besides microequilibrium dialysis and elution chromatography, a rapid anion-exchange procedure was adapted. From the concentration dependence, the $K_D$ and the binding capacity to UCP of ATP, ADP, and GTP and of the ATP analogues 5'-adenylyl imidodiphosphate (AMPPNP) and adenosine 5'-*O*-(3-thiotriphosphate) were determined. Elucidation of the pH dependence of nucleotide binding was the prime topic. From pH 4.6 to 7.5, the $K_D$ varies by almost 2 orders of magnitude, reaching the limits of the equilibrium methods. The $pK_D$ of GTP and ATP decreases from 6.3 to 4.3 with increasing pH. For ADP, the $pK_D$ varies only from 6.0 to 4.8. The intricate course of the pH dependence shows a "break point" of the $pK_D$ around pH 6.3, where the slope ($pK_D$/pH) changes between about -0.2 and -1. Another break point above pH 7.2 produces a $pK_D$/pH = -2 for ATP and GTP only. AMPPNP binding has a lower affinity ($pK_D$ about 5.8-4.1) and a pH dependence slope of -1 with no break. The breaks suggest involvement of the last ionization group ($pK_H \approx 6.7$) of the nucleotide phosphate. This agrees with the absence of a break for AMPPNP and with the shift by $Mg^{2+}$ of the break for ATP to lower pH. The best-fitting model for the pH dependence requires in addition a $H^+$ dissociating group at the binding site of UCP with a $pK_H \approx 4$, dominating the whole pH range. A second group effective above pH 7.0 amplifies the debinding specifically of ATP, not CTP or ADP. Further, the model implies binding of both $NTP^{4-}$ and the protonated $NTPH^{3-}$ or $NDP^{3-}$ and $NDPH^{2-}$ forms, however, with different affinities. On this basis, the relation between the measured overall $K_D$ and the intrinsic $K_D$'s of both nucleotide forms and the various $H^+$ dissociation constants is derived, and the corresponding $pK_D$/pH curves are calculated. A good fit with the data is obtained with a $pK_H = 3.8$ for the UCP center and a $pK_H = 6.8$ for nucleotides and with affinity ratios of 50 for $NTP^{4-}/NTPH^{3-}$ and 100 for $NDP^{3-}/NDPH^{2-}$. The binding of the protonated nucleotide $NTPH^{3-}$ is seen only at a low pH, but with the analogue $AMPPNPH^{3-}$ with $pK_H = 7.6$ it dominates the whole pH range to pH 7.2 with corresponding low affinity. Above pH 7, the dissociation of an additional group at the UCP binding center, probably histidine, is invoked. A binding site model is derived where in the nonbinding state $Glu^-$ or $Asp^-$ by an ion pair blocks $Lys^+$ or $Arg^+$ from binding the anionic nucleotides. In the binding state, $Lys^+$ or $Arg^+$ is set free on protonation of the acidic group. An additional binding regulation above pH 7.0 is interpreted due to protonation of *His*. With these two $H^+$ dissociating groups provided by the nucleotide binding site of UCP and in combination with the $H^+$ dissociation at the nucleotide, an optimized pH profile for the regulation of UCP activity in the brown fat cell is formed.

Nucleotide binding to the uncoupling protein (UCP)[1] of brown adipose tissue has been instrumental in unraveling this key element of the heat production function of the brown adipose tissue. Beginning with the finding of recoupling of respiration by addition of nucleotides to mitochondria (Rafael et al., 1969), followed by photoaffinity labeling of the 32-kDa component (Heaton et al., 1978) and subsequent isolation of UCP (Lin & Klingenberg, 1980), nucleotide binding has been the main assay for defining the protein in the mitochondria

† This work was supported by a grant from the Deutsche Forschungsgemeinschaft.

[1] Abbreviations: UCP, uncoupling protein; AAC, ADP/ATP carrier; TRA, triethanolamine; MES, 2-(*N*-morpholino)ethanesulfonic acid; PIPES, piperazine-*N*,*N*'-bis(2-ethanesulfonic acid); kDa, kilodalton(s); AMPPNP, 5'-adenylyl imidodiphosphate; ATPγS, adenosine 5'-*O*-(3-thiotriphosphate); $AP_5A$, $P^1$,$P^5$-di(adenosine-5') pentaphosphate; EDTA, ethylenediaminetetraacetic acid.

0006-2960/88/0427-0781$01.50/0 